Nuclear Instruments and Methods in Physics Research A 699 (2013) 36–40

Contents lists available at SciVerse ScienceDirect

Nuclear Instruments and Methods in Physics Research A

journal homepage: www.elsevier.com/locate/nima

Evaluation of slim-edge, multi-guard, and punch-through-protection structures before and after proton irradiation

S. Mitsui [a,*], Y. Unno [b], Y. Ikegami [b], Y. Takubo [b], S. Terada [b], K. Hara [c], Y. Takahashi [c], O. Jinnouchi [d], R. Nagai [d], T. Kishida [d], K. Yorita [e], K Hanagaki [f], R. Takashima [g], S. Kamada [h], K. Yamamura [h]

[a] The Graduate University for Advanced Studies (SOKENDAI), 1-1 Oho, Tsukuba-shi, Ibaraki-ken 305-0801, Japan
[b] Institute of Particle and Nuclear Study, High Energy Accelerator Research Organization (KEK), 1-1 Oho, Tsukuba-shi, Ibaraki-ken 305-0801, Japan
[c] Institute of Pure and Applied Sciences, University of Tsukuba, 1-1-1 Tennoudai, Tsukuba-shi, Ibaraki 305-8571, Japan
[d] Department of Physics, Tokyo Institute of Technology, 2-12-1 Okayama, Meguro-ku, Tokyo 152-8550, Japan
[e] Research Institute for Science and Engineering, Waseda University, 1-6-1 Nishi-Waseda, Shinjuku-ku, Tokyo 169-8050, Japan
[f] Department of Physics, Osaka University, Machikaneyama-cho, Toyonaka-shi, Osaka 560-0043, Japan
[g] Department of Education, Kyoto University of Education, 1 Fukakusa-Fujimori-cho, Fushimi-ku, Kyoto 612-8522, Japan
[h] Solid-state Division, Hamamatsu Photonics K.K., 1126-1 Ichino-cho, Higashi-ku, Hamamatsu-shi, Shizuoka 435-8558, Japan

ARTICLE INFO

Available online 2 June 2012

Keywords:
HL-LHC
n-in-p sensor
Slim-edge
Multi-guard ring
Punch-through-protection

ABSTRACT

Planar geometry silicon pixel and strip sensors for the high luminosity upgrade of the LHC (HL-LHC) require a high bias voltage of 1000 V in order to withstand a radiation damage caused by particle fluences of 1×10^{16} 1 MeV n_{eq}/cm^2 and 1×10^{15} 1 MeV n_{eq}/cm^2 for pixel and strip detectors, respectively. In order to minimize the inactive edge space that can withstand a bias voltage of 1000 V, edge regions susceptible to microdischarge (MD) should be carefully optimized. We fabricated diodes with various edge distances (slim-edge diodes) and with 1–3 multiple guard rings (multi-guard diodes). AC coupling insulators of strip sensors are vulnerable to sudden heavy charge deposition, such as an accidental beam splash, which may destroy the readout AC capacitors. Thus various types of punch-through-protection (PTP) structures were implemented in order to find the most effective structure to protect against heavy charge deposition. These samples were irradiated with 70 MeV protons at fluences of 5×10^{12} 1 MeV n_{eq}/cm^2–1×10^{16} 1 MeV n_{eq}/cm^2. Their performances were evaluated before and after irradiation in terms of an onset voltage of the MD, a turn-on voltage of the PTP, and PTP saturation resistance.

1. n-in-p pixel and strip sensor for ATLAS upgrade

The Large Hadron Collider (LHC) has been running at CERN in Geneva since 2009 [1]. The LHC is planned to achieve an integrated luminosity of 350 fb^{-1}. From 2022, the upgraded LHC (HL-LHC) will deliver an instantaneous luminosity 5 times as high as that of the existing LHC. A target number of the integrated luminosity is 3000 fb^{-1} at the HL-LHC. The ATLAS inner detectors will be replaced with new silicon detectors for the HL-LHC during the 2020 shutdown. In the upgraded ATLAS detector at the HL-LHC, pixel sensors placed 3.3 cm and microstrip sensors placed 30 cm from the beam pipe will be exposed to a radiation fluence of $\sim2\times10^{16}$–$\sim1\times10^{15}$ 1 MeV n_{eq}/cm^2 respectively. Therefore, we have been developing highly radiation tolerant n-in-p silicon microstrip and pixel sensors for the HL-LHC [2].

We have chosen to focus on n-in-p type sensors, since radiation damage does not reverse the bulk type. Lattice defects created by irradiation behave as p-type impurities in bulk silicon. Therefore, radiation damage only increases the p-type carrier concentration [3]. As a result, the n-in-p silicon sensor can always read signals from the strip side. Furthermore, these sensors can be operated under partial depletion conditions, because the depletion region always spreads from the readout strip side.

2. Hamamatsu sensors and proton irradiation tests

Various n-in-p test samples were fabricated by Hamamatsu Photonics K.K [4] using float-zone highly resistive silicon, FZ1 or FZ3. FZ3 has a thinner depletion region than FZ1, since FZ3 is processed with deeper backside P+ implantation. Sample dimensions are $4\times\ 4\ mm^2$ (slim-edge, multiguard) or $10\times10\ mm^2$ (PTP) with a thickness of 150, 200, or 320 μm. PTP samples also have a P-stop (P+ is implanted between strips) or P-spray (P+ is sprayed on surface) strip isolation structure for preventing from

---

[*] Corresponding author.
E-mail address: smitsui@post.kek.jp (S. Mitsui).

0168-9002/$ - see front matter © 2012 Published by Elsevier B.V.
http://dx.doi.org/10.1016/j.nima.2012.05.071

Table 1
Variety of slim-edge and multi-guard samples.

1st test, slim-edge (p-/n-edge) samples		
	200 μm	320 μm
N-bulk	FZ1	FZ1
1st test, multi-guard (p-/n-edge) samples		
	200 μm	320 μm
P-bulk	–	FZ1
N-bulk	FZ1	FZ1
2nd test, slim-edge (p-edge) samples		
	150 μm	320 μm
P-bulk	FZ1, FZ3	FZ1
P-bulk, P-spray	FZ1	FZ1
2nd test, multi-guard (p-/n-edge) samples		
	150 μm	320 μm
P-bulk	FZ1, FZ3	FZ1
P-bulk, P-spray	FZ1	FZ1

conduction between strips due to an electron accumulation layer at the Si–SiO_2 interface induced by positive charges in SiO_2 insulation layer.

We performed two proton irradiation tests with the 70 MeV beam at the Cyclotron and Radioisotope Center (CYRIC) at Tohoku University [5] (Table 1). During the first test, we irradiated the PTP, slim-edge, and multi-guard ring samples of 200 and 320 μm in thickness at 5.7×10^{12}, 1.1×10^{13}, 1.2×10^{14}, 1.2×10^{15}, and 1.1×10^{16} 1 MeV n_{eq}/cm^2. All samples were annealed at 60 °C for 80 min after irradiation. During the second test, we irradiated other slim-edge and multi-guard ring samples of 150 and 320 μm in thickness at 1.1×10^{14}, 1.2×10^{15}, 5.7×10^{15}, 1.2×10^{16} 1 MeV n_{eq}/cm^2. These samples were then annealed at 60 °C for 65 min equivalent after irradiation. The fluences of 1 MeV neutrons is estimated from multiplying the fluences of 70 MeV protons by 1/0.7 by the NIEL hypothesis.

We evaluated the full depletion voltage (FDV), energy gap (Eg) and damage constant for the PTP samples in order to estimate the consistency of the proton irradiation. FDV is estimated from body capacitance of the sensor

$$d=\sqrt{\frac{2\varepsilon V}{e}\frac{N_A+N_D}{N_AN_D}},\ C_{bulk}=\varepsilon\frac{S}{d}=S\sqrt{\frac{e\varepsilon}{2V}\frac{N_AN_D}{N_A+N_D}}.$$

where N_A is accepter density, N_D is donor density, ε is silicon permittivity, V is bias voltage, e is elementary charge, d is the depth of the depletion zone, and S is effective sensor area. The inverse square of the body capacitance, $1/C^2$, is proportional to depletion thickness. After achieving the FDV, $1/C^2$ becomes a constant, because the depth of the depletion zone, d becomes a constant. In this way, we can estimate the FDV from the $1/C^2$ curve. The FDVs for BZ4D-1 through −5 are consistent with previous measurements Fig. 1, [6].

The energy gap is obtained from the following formula:

$$I(T)=I(T_{ref})\left(\frac{1}{T_{ref}}\right)^2\exp\left(\frac{Eg}{2k_B}\left(\frac{1}{T}-\frac{1}{T_{ref}}\right)\right).$$

where Eg is the energy gap, k_B is the Boltzmann constant, T is temperature, T_{ref} is reference temperature, and I is leakage current. Eg is calculated from the leakage currents at the FDV at a certain temperature [7]. We measured the PTP samples irradiated at 1.2×10^{15} 1 MeV n_{eq}/cm^2 at −60, −50, −40, −30, and −20 °C. T_{ref} was 20 °C. Eg was found to be 1.21 eV (Fig. 2).

The damage constant α is calculated from

$$\Delta I=\alpha\times V\times\Phi.$$

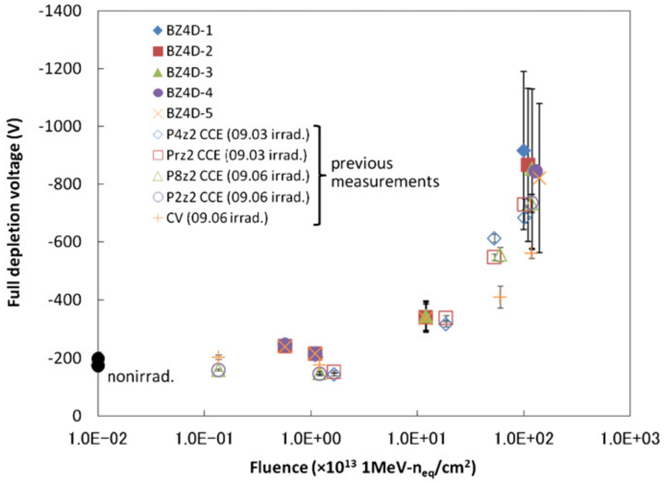

Fig. 1. Comparison of the Full Depletion Voltage for present and previous measurements.

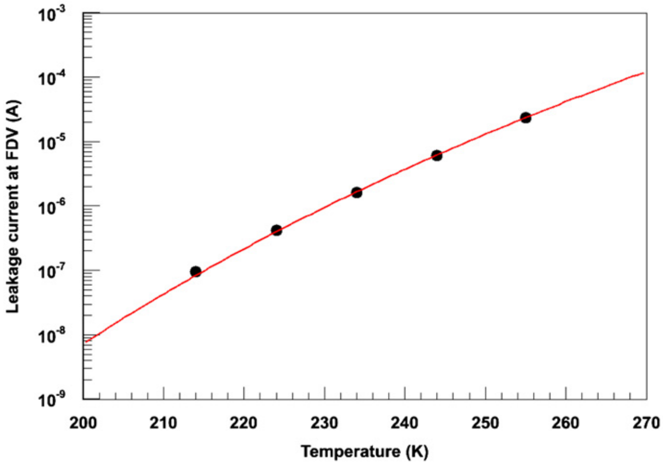

Fig. 2. Temperature dependence of leakage current in BZ4D-5 irradiated at 1×10^{15}; 1 MeV n_{eq}/cm^2.

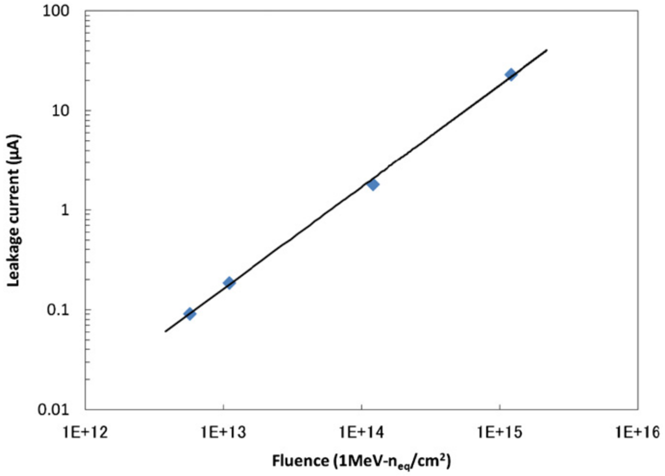

Fig. 3. Fluence dependence of leakage current in PTP samples.

where ΔI is leakage current, V is effective sensor volume, Φ is the fluence. For a PTP sample irradiated at 1.2×10^{15} 1 MeV n_{eq}/cm^2 at the FDV, the effective sensor volume is estimated to be $0.772\ cm^2\times0.032$ cm. The damage constant at the FDV is then estimated as 4.6×10^{-17} A/m before annealing (Fig. 3).

3. Slim-edge

We examined slim edge samples in order to find the minimal edge width able to withstand a bias voltage of up to 1000 V for minimizing the inactive area of the silicon sensor. MD caused by an avalanche of electrons occurs from the high electric field developed as the depletion region spreads from the implant electrodes to the dicing edge.

At one side, edge width from the bias ring to the dicing edge was varied from 80 to 964 μm. P^+ or N^+ regions are implanted around the surface of the sensor edge. We examined p-bulk and n-bulk sensors with p-edge or n-edge investigating whether the p–n junction in the edge region affects the bias voltage tolerance. We measured the leakage current as a function of the bias voltage (*IV* curve) for 0 to -2000 V at $-20\,^{\circ}$C. We define the onset voltage for MD as the point where the slope of the *IV* curve becomes 5 times larger than the smallest slope in the lower voltage region [8].

In Fig. 4 the abscissa shows the field width (the width from the bias ring to the dicing edge without implantations) and the ordinate shows the onset voltage for MD. The n-bulk n-edge sensor breaks down less than 700 V, because a p–n junction exists between the edge implantation and the bulk. We infer that the n-bulk substrate changes to p-type through an irradiation fluence in excess of 1×10^{14} 1 MeV n^{eq}/cm^2, while the surface is still n-type. The n-bulk p-edge samples have no p–n junction. Therefore, these samples show good bias voltage tolerance, although the onset voltages of MD are about 700 V. We see that onset voltage for MD increases with field width until about 400 μm, after which onset voltage becomes constant. The n-bulk or p-bulk (200 or 320 μm in thickness) may require ≥ 450 μm field width to withstand 1000 V (Fig. 5). In Fig. 6, six samples have the same field width of 230 μm with different edge widths. As each sample breaks down at the same bias voltage, we conclude that the onset voltage for MD is independent of the edge width.

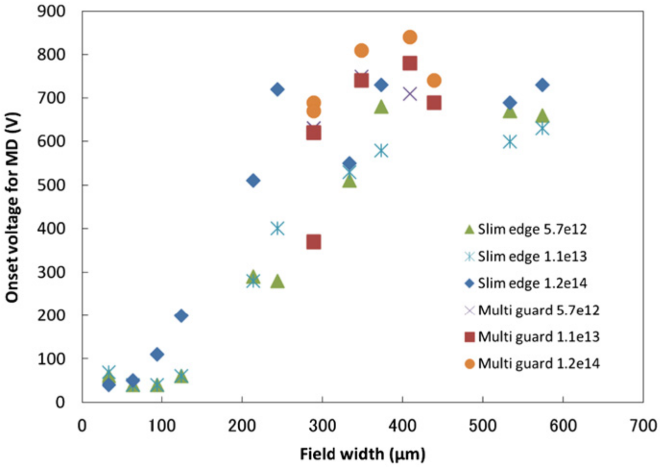

Fig. 4. Field width dependence of the onset voltage for MD.

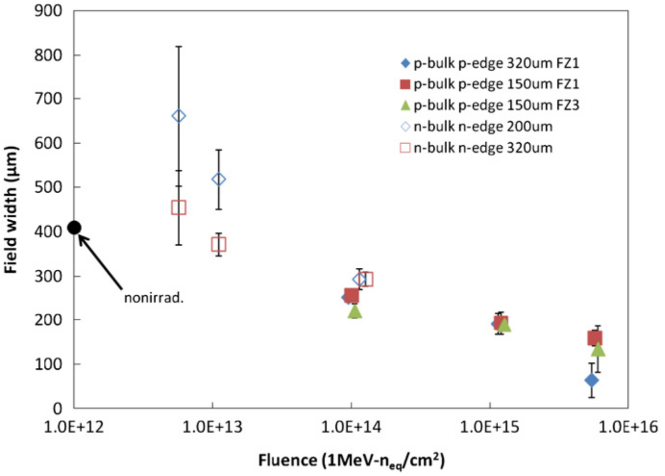

Fig. 5. Fluence dependence of field width hold up to 1000 V.

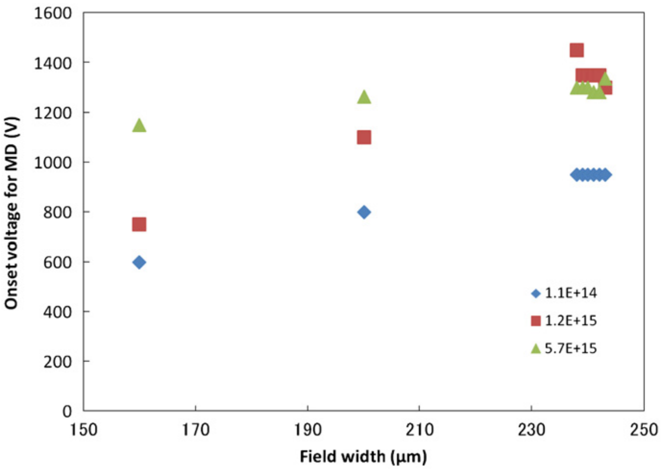

Fig. 6. Field width dependence of onset voltage for MD for a p-bulk, p-edge sample with 320 μm thickness.

Fig. 7. Structure of multi guard ring.

4. Multiguard

Guard rings are implanted around the bias ring in order to prevent high voltage break down around the edge by weakening the electric field. We investigated the various edge configurations, the number of guard rings, and the width of the guard ring in order to find the minimal overall edge width for withstanding 1000 V. We examined p-bulk and n-bulk sensors with 6 types of multi guard ring structures, 1GR-narrow, 1GR-middle, 1GR-wide, 2GR-middle, 2GR-wide and 3GR-wide (Fig. 7). Each sample has the same field width of 350 μm. We measured leakage current by applying a bias voltage of 0 to -2000 V at $-20\,^{\circ}$C and estimated the onset voltage for MD in a manner as described previously [8].

Fig. 8 shows the MD onset voltage as a function of fluence. Before irradiation, the multi GR (2GR, 3GR) withstands a higher bias voltage than the single GR. After irradiation, however, no

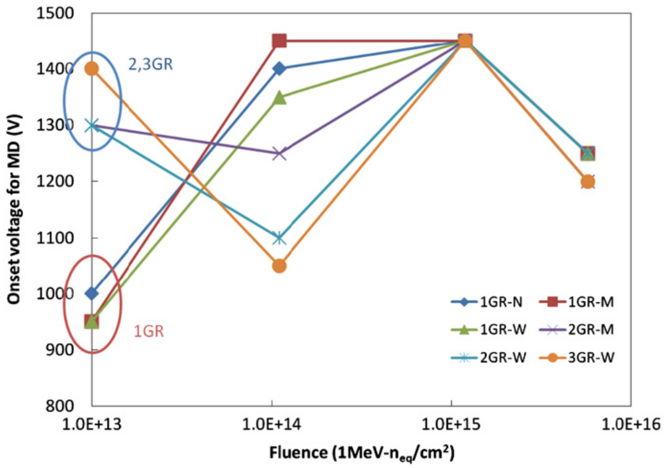

Fig. 8. Fluence dependence of onset voltage for MD for FZ1 p-bulk sample with 150 μm thicknessc.

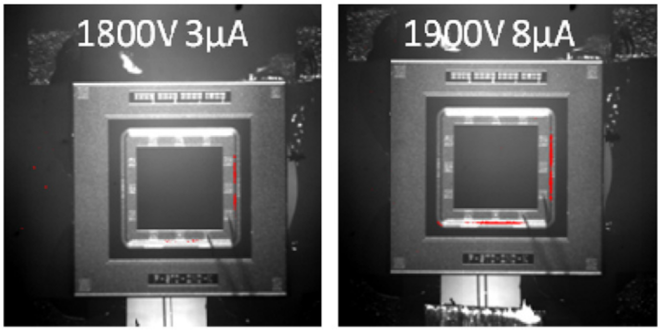

Fig. 9. Hot electron photograph at 1800 V and 1900 V.

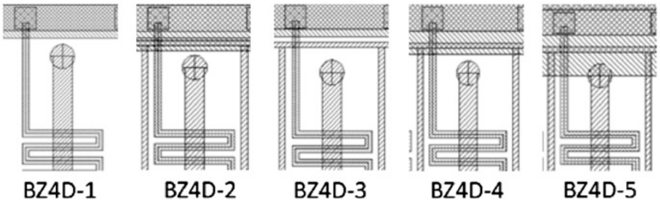

Fig. 10. PTP types of bias Al extension. Only one side is extended.

difference is apparent. Both the 150 and 320 μm thick samples (FZ1 and FZ3) behave the same way.

4.1. Hot electron photograph

Using hot electron photographs, we identified the hot spot location caused by the MD. A back-thinned cooled CCD camera having infrared sensitivity can image any hot spots caused by MD. Fig. 9 shows the hot spots for multi guard samples with the bias voltage of 1800 V and 1900 V. Break-down at the bias ring occurs first. As bias voltage increase further the guard ring then breaks down. This phenomenon is common to all samples regardless of the number and width of the guard rings.

5. Novel punch-through-protection (PTP)

PTP structures should protect the AC coupling capacitors, for which break down voltage is designed to be ~120–150 V. This break voltage may be surpassed by a large induced charge from e.g. an accidental beam splash. The PTP structure is to mitigate the situation by discharging directly to the bias ring. Test samples are p-bulk sensors of 320 μm in thickness. As shown in Fig. 10, we

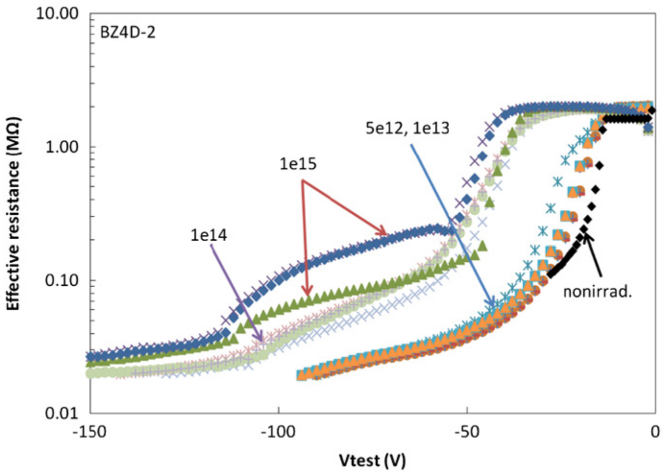

Fig. 11. Effective resistance for BZ4D-2 irradiated at up to ~1×10^{15} n$_{eq}$/cm^2.

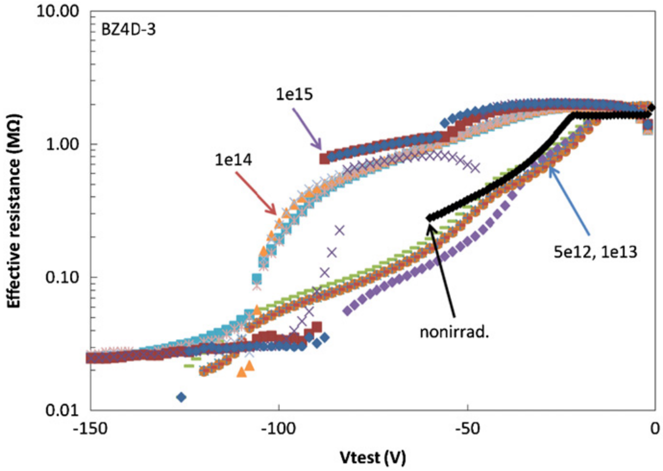

Fig. 12. Effective resistance for BZ4D-3 irradiated at up to ~1×10^{15} n$_{eq}$/cm^2.

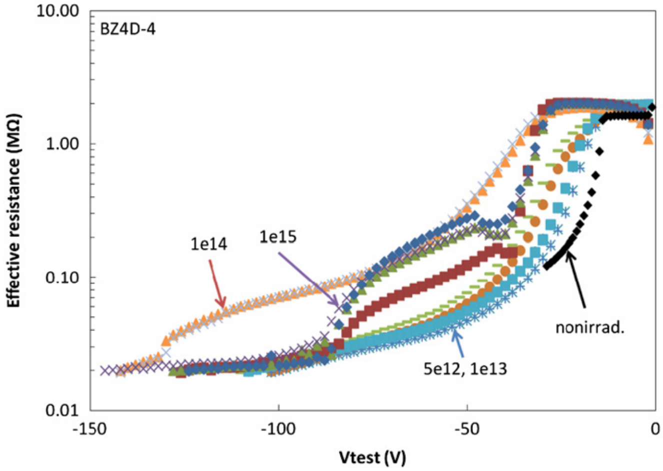

Fig. 13. Effective resistance for BZ4D-4 irradiated at up to ~1×10^{15} n$_{eq}$/cm^2.

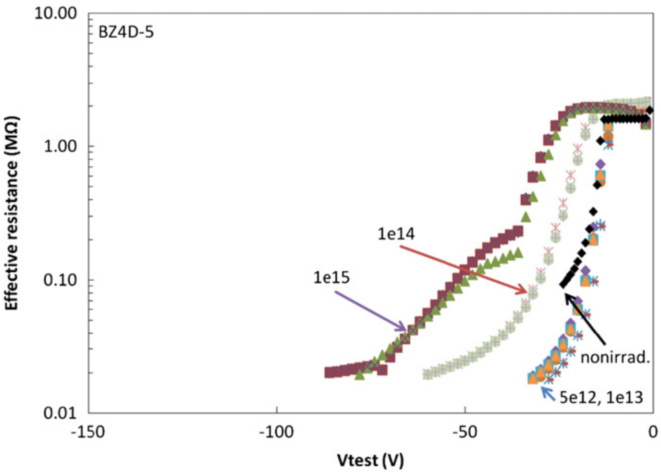

Fig. 14. Effective resistance for BZ4D-5 irradiated at up to $\sim 1\times 10^{15}$ n_{eq}/cm^2.

considered 5 kinds of structures with various Al width extended from the bias ring and with or without a p-stop:

BZ4D-1: no Al extension, no p-stop
BZ4D-2: Al extension up to p-stop
BZ4D-3: no Al extension, p-stop
BZ4D-4: Al extension over p-stop
BZ4D-5: full Al extension with p-stop

We measured the resistance between the bias ring and the DC pad connected to the n-strip implant by applying a voltage, *V* test, until the effective resistance became as low as 20 kΩ otherwise at most -150 V [9]. When the PTP structure is inactive the effective resistance is about 1.5 MΩ, which corresponds to the resistance of the bias resistor. After the PTP becomes active, the effective resistance decreases (Figs. 11–14). The punch-though voltage, *V*pt, is defined as the voltage where the bias resistance decreases by half. As the fluence increases, the onset voltage and *V*pt increases (Figs. 11–14). BZ4D-5 performs the best, showing a lower *V*pt, a sharper cutoff, and a lower saturation resistance. A wider Al extension shows a lower Vpt and a lower saturation resistance. With the full Al extension, *V*pt <100 V with a saturation resistance ≤ 20 kΩ and ~ 5 mA per strip (equivalent to ~ 10 kMIPS/25 ns/strip). BZ4D-5 can protect the AC coupling capacitor against an accidental beam splash.

6. Conclusions

We have evaluated radiation tolerance of n-in-p sensors with a planar geometry by irradiating various samples at fluences of up to 1×10^{16} 1 MeV n_{eq}/cm^2. We examined slim-edge samples with a narrow edge width for minimizing the ineffective area of the silicon sensor. A large field width leads to a higher bias voltage tolerance. Both n-bulk and p-bulk require a field width ≥ 450 μm in order to withstand 1000 V. The MD onset voltage was found to be independent of the edge width.

We investigated whether the number of guard rings and the width of the guard ring help reduce the overall edge width. With increasing number of guard rings, bias voltage tolerance improved before irradiation. With increasing bias voltage, bias ring break-down occurs first, followed by guard ring break-down.

We evaluated novel PTP structures and found that BZ4D-5 (with full extension of the bias ring width) performed the best. This structure should be able to protect the AC coupling capacitor even after an irradiation of 1×10^{15}1 MeV n_{eq}/cm^2.

References

[1] ATLAS Collab, Journal of Instrumentation 3 (2008) S08003.
[2] Y. Unno, et al., Nuclear Instruments and Methods in Physics Research A 636 (2011) S24.
[3] M. Moll, Radiation Damage in Silicon Particle Detectors, Ph. D. Dissertation, Hamburg University, 1999.
[4] K.K. Hamamatsu Photonics, 1126-1 Ichino-cho, Hamamatsu-shi, Shizuoka 435-8558, Japan.
[5] Experiment no. 9362, CYRIC, Aoba 6-3, Aoba-ku, Sendai-shi, Miyagi 980-8578, Japan, February 2011.
[6] K. Hara, et al., Nuclear Instruments and Methods in Physics Research A 636 (2011) S83.
[7] E. Barberis, et al., Nuclear Instruments and Methods in Physics Research A 326 (1993) 373.
[8] Y. Unno, et al., Nuclear Instruments and Methods in Physics Research A 650 (2011) 129.
[9] H.F.-W. Sadrozinski, et al., Nuclear Instruments and Methods in Physics Research A 658 (2011) 46.